Moisture Desorption Studies on Polymer Hydrated and Vacuum Extruded Bentonite Clay Mat

Eric Wooi Kee LOH[1], Devapriya Chitral WIJEYESEKERA[2], Mihaela Anca CIUPALA[3]

[1] *Faculty of Built Environment, Linton University College, Negeri Sembilan, MALAYSIA*

Address: Persiaran UTL, BUTL, Batu 12, 71700 Mantin, Negeri Sembilan, Malaysia

Tel. +606 758 7888; Fax +606 758 7599; email: ericdrloh@gmail.com

[2] *Faculty of Civil & Environmental Engineering, Universiti Tun Hussein Onn Malaysia, Johor, MALAYSIA*

Address: 86400 Batu Pahat, Johor, Malaysia

Tel. +607 456 4484; email: dcwijey@gmail.com

[3] *School of Architecture, Computing and Engineering, University of East London, London, UNITED KINDOM*

Address: University Way, London E16 2RD, United Kingdom

Tel. +44 (0) 20 8223 2528; email: m.a.ciupala@uel.ac.uk

Acknowledgement: This work was supported by the Knowledge Transfer Partnerships under Grant: KTP000320

Abstract: Moisture desorption observations from two bentonite clay mats subjected to ten environmental zones with individually different combinations of laboratory controlled constant temperatures (between 20^0C to 40^0C) and relative humidity (between 15% to 70%) are presented. These laboratory observations are compared with predictions from mathematical models, such as Thin-layer drying equations and kinetic drying models proposed by Page, Wang and Singh, and Henderson and Pabis. The quality of fit of these models is assessed using standard error of estimate, relative percent of error and coefficient of correlation. The Page model was found to better predict the drying kinetics of the bentonite clay mats for the simulated tropical climates. Critical study on the drying constant and moisture diffusion coefficient help to assess the efficacy of a polymer to retain moisture and control desorption through water molecule bonding. This is further substantiated with the Guggenheim-Aderson-DeBoer (GAB) desorption isotherm model which is presented.

Key Words: Bentonite clay mat, Controlled environment, Moisture desorption, Drying constant, Moisture diffusion coefficient

1. Introduction

The industrial application of bentonite clay mats as waste containment barriers requires them to have minimal desorption characteristics. The polymer hydration and vacuum extrusion process create a clay with suitable consistency properties and an oriented bentonite clay microstructure coupled with an efficient double layer (Schroeder, et al., 2001; Kolstad, et al., 2004; Di-Emidio, et al., 2008; Katsumi, et al., 2008; Wijeyesekera, et al., 2012; Loh and Wijeyesekera, 2015).

Numerous reported studies on convection drying of clay are based on mathematical models for describing the kinetics of this process. Fick's laws of diffusion and Fourier's law of conduction as well as its derived equation (e.g. Thin-layer drying equation) account for a significant proportion of the mathematical models employed in clay science (Evans and Keey, 1975; Tomas, et al., 1993; Kanno, et al., 1996; Su 1997; Sander, et al., 1998, 2001, 2003; Moropoulou, et al., 2004, 2005; Murugesan, et al., 2001; Mihoubi, et al., 2004; Dincer and Sahin, 2004; Akpinar and Dincer, 2005; ; Chemkhi, et al., 2004, 2005). However, many of these models include different moisture transfer parameters that have a wide variation of reported values, depending on the complexity of the product and methods of moisture estimation.

The modelling of the drying process is very often described in the literature through moisture sorption isotherm models. An isotherm obtained by exposing a solid to air of increasing humidity gives the adsorption isotherm, whilst the isotherm obtained by exposing a solid to air of decreasing humidity is known as the desorption isotherm. The latter is of particular interest in clay drying as the moisture content of the solid materials progressively decreases when exposed to various climatic conditions. There are several models available in the literature to describe the moisture sorption isotherm. They can be divided into several categories: (a) kinetic models based on a mono-layer, such as the BET model (Brunauer et al., 1938), (b) kinetic models based on a multi-layer and condensed film, such as the GAB model (Van den Berg & Bruin, 1981), (c) semi-empirical models (Henderson, 1952; Halsey, 1948; Chung and Pfost, 1967) and (d) empirical models (Smith, 1947; Oswin, 1946). However, no model accurately fits sorption isotherm data for different moist products over a broad range of relative humidity and temperature. This is attributed to the fact that the sorption isotherm of each moist product is influenced by integrated hygroscopic properties of its numerous constituents and that the depression of water activity is due to a combination of factors, each of which could be predominant in a given range of water

activity in the system. Therefore, there is a clear need to develop an improved conceptual understanding of the drying behaviour of bentonite clay mat during the desorption process.

2. Materials and Methods

Two sets of polymer hydrated and vacuum extruded bentonite clay mat, nominally coded as TSA and TSB were used in this study. A target moisture content of circa 40% was achieved by mixing the bentonite with a dilute polymeric solution containing different ratio of sodium carboxymethyl cellulose, polyacrylate and propylene glycol in a high speed and high shear mixer, provided with rotary blades and a turning pan. One of the primary purposes of the liquid polymer treatment is to improve the rheological properties of the clay mats as well as to control the moisture migration. The exact mix proportions are not disclosed for commercial reasons.

The X-ray diffraction (XRD) analysis showed the clay mineralogy of the bentonite to be smectite (93%), quartz (2%), feldspars (4%) and gypsum (1%). Bulk sample of these bentonite was analysed and shown to be composed of 87.5% of particles that were within a size range less than 75μm and had an air dried moisture content of 10 -14% by weight (the moisture being absorbed from the atmosphere). The chemical composition of both TSA and TSB specimens as obtained using X-ray Florescence (XRF) analyser shown to be composed Na_2O (1.99%), MgO (2.32%), Al_2O_3 (18.29%), SiO_2 (79.05%), K_2O (0.37%), CaO (1.6%), TiO_2 (0.22%), Fe_2O_3 (4.56%).

The experiments were performed in an environmental chamber (see Fig. 1) with a purpose built arrangement to control the desired temperature and relative humidity as shown in Table 1. A 5mm thick, 100mm diameter, cylindrical specimen of the bentonite clay mat was placed on the specimen holder and allowed to dry isothermally under preset conditions. The changes in mass of

95 the specimen with time were monitored using a digital balance linked to a computer facilitating
96 regular data acquisition and monitoring. Air temperature and relative humidity were measured
97 through the use of a pre-calibrated semiconductor sensor. The accuracy of the respective
98 observed measurements was as follows: 0.01g for mass, 0.1ºC for temperature and 0.1% for the
99 relative humidity. The variations in the moisture content observation during the isothermal drying
100 of the specimen was correlated with the following four published mathematical models:

101 **i. Wang & Singh** (Wang & Singh, 1978) − Model I

102 $$X = \left(X_0 - X_{eq}\right)\left(1 + at + bt^2\right) + X_{eq} \quad (1)$$

103 **ii. Henderson & Pabis** (Guarte, 1996) − Model II

104 $$X = \left(X_0 - X_{eq}\right).\beta e^{-k.t} + X_{eq} \quad (2)$$

105 **iii. Thin layer equation** (Jayas, 1991) − Model III

106 $$X = \left(X_0 - X_{eq}\right)e^{-k.t} + X_{eq} \quad (3)$$

107 **iv. Page** (Jayas, 1991) − Model IV

108 $$X = \left(X_0 - X_{eq}\right)e^{-k.t^n} + X_{eq} \quad (4)$$

109 The quality of the fitting was evaluated by calculating the mean relative percent error (P),
110 standard error (SE) and the coefficient of correlation (R^2) between the experimental (y_{exp}) and
111 predicted data (y_{cal}).

112 $$P = \frac{100}{N}\sum_{j=1}^{N}\left|\frac{y_{jcal} - y_{j\exp}}{y_{j\exp}}\right| \quad (6)$$

113 $$SE = \sqrt{\sum_{j=1}^{N}\frac{\left(y_{jcal} - y_{j\exp}\right)^2}{N - n_p}} \quad (7)$$

114 $$R^2 = \frac{S_t - SSE}{S_t} \quad (8)$$

where,

$$S_t = \sqrt{\frac{\sum_{j=1}^{N}\left(\bar{y} - y_j\right)^2}{n-1}} \quad (9)$$

$$\bar{y} = \frac{\sum_{j=1}^{N} y_j}{N} \quad (10)$$

$$SSE = \sum_{j=1}^{N}\left(y_{jcal} - y_{j\exp}\right)^2 \quad (11)$$

3. Results and Discussion

3.1 Best Fit Drying Kinetic Models

Experimental drying data for TSA specimen obtained from the 'C0' environmental condition (temperature = 40°C and relative humidity = 15%) was chosen and the observed outputs from this condition are presented in Fig. 2, while the outputs for other environmental conditions tabulated in Table 2 are also presented for completeness. As shown in Fig. 2, the quality fitting parameters demonstrated that all models reproduce experimental data with great accuracy ($0.9723 < R^2 < 0.9998$). The standard error (SE) and mean relative error for MODEL I is 1.2179 and 3.5183, and the coefficient of correlation R^2 value between the experimental value and predicted value is 0.9723. It is noteworthy that for the MODELS II and III, the same values of 2.1259, 0.4133 and 0.9968 are obtained for *%P, SE* and R^2 parameter respectively. This suggests that the parameter β does not a significant influence on the moisture content of TSA and TSB specimens, for the range of temperature and relative humidity considered in this study. The MODEL IV gave the most desirable *%P*, *SE* and R^2 values compared to the other models, in particular in the highest coefficient of correlation R^2 value (0.9998) as well as the lowest *%P*

(0.9063) and *SE* (0.1016) value. Furthermore, MODELS I, II and III gave some residual values which are much larger than any other fitted points at the initial drying state which overcompensated the moisture content. This phenomenon is more pronounced in MODEL I. Thus this suggests that the aforementioned models are not sufficiently predictive over the range of experimental data. Over and above, evidences from the results for others thermal environment (see Table 2) also made MODEL IV favourable to be the most appropriate regression model.

3.2 Drying Constants

The drying constants k and n in the Page equation are essentially functions of transport properties. The influence of the thermal environment condition on these parameters is analysed and presented in Figs. 3 to 6 for TSA and TSB specimens respectively. For the considered ranges of temperature, an increase in the relative humidity causes a maximum reduction of circa 82% and 83% was noted for the parameter k in TSA and TSB specimens, respectively. This phenomenon is more pronounced in the higher temperature range. Conversely, the sensitivity of parameter k to temperature apparently reveals that at a lower relative humidity range. It was observed that the increase in temperature resulted a maximum increment of circa 55% and 300% for the parameter k in TSA and TSB specimens. There was no significant correlation between parameter n on the thermal environment noted from the present study. Similar observation was also reported by Sander et al. (1998 & 2003) for thin plates of illite montmorillonite clay. Sander had concluded that the parameter n is independent of the drying conditions.

3.3 Moisture Diffusion Coefficient:

For a drying process devoid of a constant rate period is observed, such as in the present case. It could then be assumed that internal diffusion prevails as a mechanism of matter transfer.

Therefore, moisture diffusivity can be calculated from the experimental drying data using Fick's second law (Sander et al., 1998). According to Geankoplis (1983), the solution to the diffusion equation for thin plate shaped material drying from one surface is:

$$\psi = \frac{X - X_{eq}}{X_0 - X_{eq}} = \frac{8}{\pi^2} \cdot e^{\left(\frac{-\pi^2 \cdot D_{eff} \cdot t}{L^2}\right)} \quad (12)$$

Comparing the effective diffusion coefficients from Figs. 7 and 8, it is evident that they differ substantially under similar thermal environment conditions. It is observed that with TSA specimen, the moisture diffusivity is higher and this trend is consistent with the experimental observations. A plausible explanation for this deviation is the consequence of the higher biding energy of the polymer properties in TSB specimen. This finding is further supported by the evidence from desorption isotherm model.

3.4 Desorption Isotherm

The knowledge of the desorption isotherm portrays the hygroscopic equilibrium of moisture at varies temperature in the product, is essential in the study of the effects of drying of the clay mat. Experimental data on these isotherms at temperature from 20 to 40°C and water activity from 0.20 to 0.70 were determined using the static gravimetric method. The experimental data were fitted by the well-known Guggenheim-Anderson and de Boer (GAB) model (Van den Berg & Bruin, 1981):

$$X = \frac{X_m C K A_w}{(1 - K A_w)(1 - K A_w + C K A_w)} \quad (13)$$

Figs. 9 to 11 present the experimental desorption isotherms for both TSA and TSB specimen at temperatures of 20, 30 and 40°C respectively. In these figures, *EMC* is the equilibrium moisture content of the specimen expressed on a dry mass basis (kg water per kg of dry clay) and

181 A_w is the water activity, defined as the ratio of the partial pressure, P to the saturated vapour
182 pressure, P_0 at the temperature of equilibrium and expressed as:

183 $$A_w = \frac{p}{p_0} \quad (14)$$

184 It is seen and noted from these figures that: (i) the isotherms are of the normal S-type
185 following the Brunauer (1945) classification; (ii) the *EMC* of both specimens decreases with the
186 increases in temperature; (iii) the *EMC* of TSA specimen varies from 0.0 to 0.18 $kg.kg^{-1}$, but for
187 TSB specimen varies from 0.0 to 0.31 $kg.kg^{-1}$; (iv) notable difference exists between *EMC* of
188 TSA and TSB specimen, at a given temperature. The last observation may be explained by the
189 higher polarity of water molecules and the tendency for better hydrogen bonding. This implies
190 that desorption of moisture from TSB specimen may be more difficult than from TSA specimen.
191 As a consequence, the physical desorption of moisture is reduced. This effect is uniquely
192 responsible for the proportional of polymer properties in the TSB specimen. To substantiate the
193 aforesaid, the sorption capacity of monolayer moisture content was investigated. The value of the
194 monolayer moisture content (X_m) obtained by the GAB model is an important parameter. It is
195 regarded as the sorption capacity of the adsorbent and the indicator for available polar sites of
196 binding water vapour (Chung & Pfost, 1967 as cited by Mihoubi & Bellagi, 2006). As shown in
197 Table 3, the monolayer moisture content values of TSA specimen ranged from 5.80% to 7.40%
198 d.b. and 7.41% to 9.92% d.b. for TSB specimen in the temperature ranges of 20 to 40°C. It was
199 noteworthy that the monolayer moisture content values of TSB specimens were higher than those
200 of the TSA specimens at all temperatures. This is a further demonstration of the improvement of
201 the water molecules binding in TSB specimen.
202

203 ## 4. Conclusion:

The purpose built environmental chamber provided representative observations to study the drying characteristic of two set of polymer hydrated and vacuum extruded bentonite clay mats when subjected to ten different thermal environments. The exclusively high correlation of the Page model to the experimental drying data justified the mathematical model for describing the drying kinetics of the clay mats in an isothermal drying condition. The influence of temperature and relative humidity level on the transport properties, such as drying constant, moisture diffusion coefficient and exponential model parameter were estimated. The research further provided a means of quality control assessment in defining the TSB specimen have a higher water molecule bonding capacity and lower desorption characteristics compared with the TSA specimen.

5. Notations:

A_w - water activity [%]

C - parameter in model

D_{eff} - effective diffusivity at the drying temperature [m^2/s]

K - parameter in model

L - thickness of the slices [m]

X - moisture content [%]

X_0 - initial moisture content [%]

X_{eq} - equilibrium moisture content [%]

X_m - monolayer moisture content

a - parameter in model

b - parameter in model

227 k - parameter in model [s^{-1}]

228 n - parameter in Model [s^{-1}]

229 t - drying time [s]

230 w - material moisture content [%]

231 β - parameter in model

232 ψ - dimensionless moisture content

233

234 ## References:

235 Akpinar, E.K., and Dincer, I. (2005). “Moisture transfer models for slabs drying”.
236 International Communications in Heat and Mass Transfer, Vol. 32, No. 1, pp. 80-93, DOI:
237 10.1016/j.icheatmasstransfer.2004.04.037.

238 Brunauer, S., Emmett, P.H., and Teller, E. (1938). “Adsorption of gases in multi-molecular
239 layers”. Journal of the American Chemical Society, Vol. 60, No. 2, pp. 309–319, DOI:
240 10.1021/ja01269a023.

241 Chemkhi, S., and Zagrouba, F. (2005). “Water diffusion coefficient in clay material from
242 drying data”. Desalination, Vol. 185, No. 1, pp. 491–498, DOI: 10.1016/j.desal.2005.04.052.

243 Chemkhi, S., Zagrouba, F., and Bellagi, A. (2004). “Thermodynamics of water sorption in
244 clay”. Desalination, Vol. 166, No. 1, pp. 393-399, DOI: 10.1016/j.desal.2004.06.094.

245 Chung, D.S., and Pfost, H.B. (1967). “Adsorption and desorption of water vapour by cereal
246 grains and their products. Part II: Development of the general isotherm equation”. Transactions of
247 the ASABE, Vol. 10, No. 4, pp. 552–555. DOI: 10.13031/2013.39727

Di Emidio, G., Mazzieri, F., and Van Impe, W. (2008). “Hydraulic Conductivity of a Dense Prehydrated GCL: Impact of Free Swell and Swelling Pressure”. Proc. 4th European Geosynthetics Conference, Golder Associates, Nottingham, UK, Paper No 320.

Dincer, I., and Sahin, A.Z. (2004). “A new model for thermodynamic analysis of a drying process”. International Journal of Heat and Mass Transfer, Vol. 47, No. 4, pp. 645–652, DOI:10.1016/j.ijheatmasstransfer.2003.08.013

Evans, A.A., and Keey, R.B. (1975). “The moisture diffusion coefficient of a shrinking clay on drying”. The Chemical Engineering Journal, Vol. 10, No. 1, pp. 127-134 DOI:10.1016/0300-9467(75)88027-0

Geankoplis, C.J. (1993). Transport Processes and Unit Operation, 3rd Edition, Prentice Hall, Englewood Cliffs.

Guarte, R.C. (1996). Modelling the drying behaviour of copra and development of a natural convection dryer for production of high quality copra in the Philippines. Ph.D. thesis, Hohenheim University, Germany.

Halsey, G. (1948). “Physical adsorption on non-uniform surfaces”. Journal of Chemistry and Physics, Vol. 16, No. 10, pp. 931–937, DOI: 10.1063/1.1746689.

Henderson, S.M. (1952). “A basic concept of equilibrium moisture”. Agricultural Engineering, Vol. 33, No. 1, pp. 29–32, DOI: -

Jayas, D.S., Cenkowski, S., Pabis, S., and Muir, W.E. (1991). “Review of thin-layer drying and wetting equations”. Drying Technology, Vol. 9, No. 3, pp. 551-588, DOI: 10.1080/07373939108916697.

Katsumi, T., Ishimori, H., Onikata, M., and Fukagawa, R. (2008). “Long-term barrier performance of modified bentonite materials against sodium and calcium permeant solutions”. Geotextiles and Geomembranes, Vol. 26, pp. 14-30, DOI:10.1016/j.geotexmem.2007.04.003.

272 Kolstad, D.C., Benson, C.H., Edil, T.B., and Jo, H.Y. (2004). “Hydraulic conductivity of a
273 dense prehydrated GCL permeated with aggressive inorganic solutions”. Geosynthetics
274 International, Vol. 11, No. 3, pp. 233-241, DOI: 10.1680/gein.2004.11.3.233.
275 Loh, E.W.K., and Wijeyesekera, D.C. (2015). “Hydraulic Flow through Engineering
276 Bentonite-Based Containment Barriers”. American Journal of Applied Sciences. Vol. 12, No. 11,
277 pp. 785-793, DOI: 10.3844/ajassp.2015.785.793.
278 Mihoubi, D., and Bellagi, A. (2006). “Thermodynamic analysis of sorption isotherms of
279 bentonite”. Journal of Chemical Thermodynamics, Vol. 38, No. 9, pp. 1105-1110,
280 DOI:10.1016/j.jct.2005.11.010
281 Mihoubi, D., Zagrouba, F., and Bellgi, A. (2002). “Drying of Clay. I: Material
282 Characteristics”. Drying Technology, Vol. 20, No. 2, pp. 465-487, DOI: 10.1081/DRT-
283 120002552.
284 Murugesan, K., Suresh, H.N., Seetharamu, K.N., Narayana, P.A.A., and Sundararajan, T.
285 (2001). “A theoretical model of brick drying as a conjugate problem”. International Journal of
286 Heat and Mass Transfer, Vol. 44, No. 21, pp. 4075-4086, DOI: 10.1016/S0017-9310(01)00065-5.
287 Oswin C.R. (1946). “The kinetics of package life. III. Isotherm”. Journal of the Society of
288 Chemical Industry, Vol. 65, No. 12, pp. 419–421, DOI: 10.1002/jctb.5000651216
289 Sander, A., Kardum, J. P., and Skansi, D. (2001). “Transport Properties in Drying of Solids”.
290 Chemical and Biochemical Engineering Quarterly, Vol. 15, No. 3, pp. 131-137, DOI: -
291 Sander, A., Skansi, D., and Bolf, N. (2003). “Heat and mass transfer models in convection
292 drying of clay slabs”. Ceramics International, Vol. 29, No. 6, pp. 641–653, DOI: 10.1016/S0272-
293 8842(02)00212-2.

294 Sander, A., Tomas, S., and Skansi, D. (1998). “The influence of air temperature on effective
295 diffusion coefficient of moisture in the falling rate period”. Drying Technology, Vol. 16, No. 7,
296 pp. 1487-1499, DOI: 10.1080/07373939808917472
297 Schroeder, C., Monjoie, A., Illing, P. Dosquet, D., and Thorez, J. (2001). “Testing a Factory-
298 Prehydrated GCL under Several Conditions”. Proc., 8th International Waste Management and
299 Landfill Symposium, CISA, Cagliari, Italy, Vol.1, pp. 188-196.
300 Smith, S.E. (1947). “The sorption of water vapour by high polymers”. Journal of the
301 American Chemical Society, Vol. 69, No. 3, pp. 646-651, DOI: 10.1021/ja01195a053.
302 Tomas, S., Skansi, D. & Sokele, M. (1993). “Kinetics of the clay roofing tile convection
303 drying”. Drying Technology, Vol. 11, No. 6, pp. 1353-1369, DOI: 10.1080/07373939308916903.
304 Van den Berg, C., Bruin, S. (1981). “Water activity and its estimation in food systems:
305 Theoretical aspects”. In: Rockland, L.B. & Stewards, G.F., Eds. Water activity. Influence on food
306 quality, Academic Press, New York, pp. 1–61.
307 Wang, C.Y. and Singh, R.P. (1978). “A single layer drying equation for rough rice”. ASAE
308 Paper No. 3001. St.Joseph.
309 Wijeyesekera, D.C., Loh, E.W.K., Siti, F.D., Lim, A.J.M.S., Zainorabidin, A.B., Ciupala,
310 M.A., (2012). “Sustainability Study of the Application of Geosynthetic Clay Liners in Hostile
311 and Aggressive Environments”. OIDA International Journal of Sustainable Development. Vol. 5,
312 No. 6, pp. 81-96. DOI: -

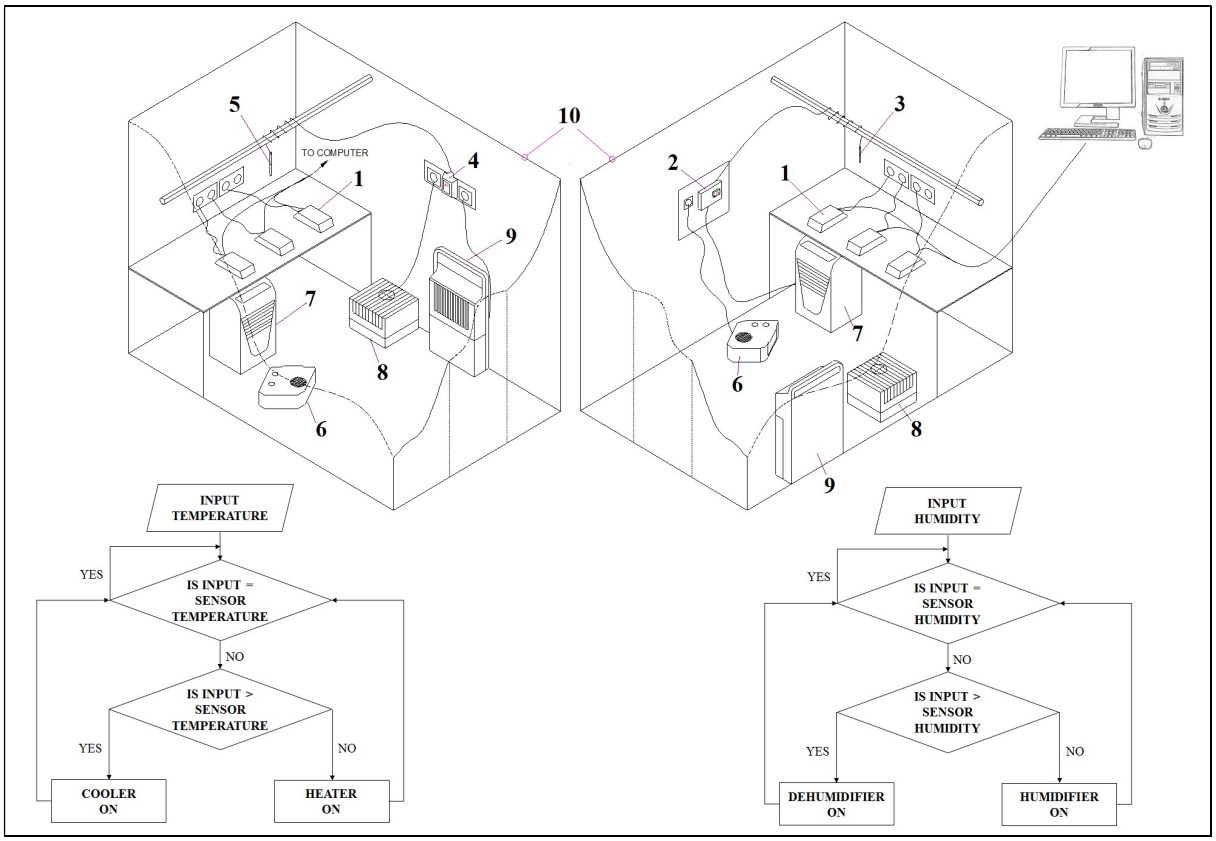

Fig. 1. Schematic diagram of the environmental chamber and the ancillary equipments for the convective drying: 1 – Electronic Balances (Suite of 3 Specimens); 2 – Temperature Controller / Data Logger; 3 – Temperature Sensor; 4 – Himidity Controller / Data Logger; 5 – Humidity Sensor; 6 – Heater; 7 – Cooler; 8 – Humidifier; 9 – Dehumidifier; 10 – Wall with Insulation.

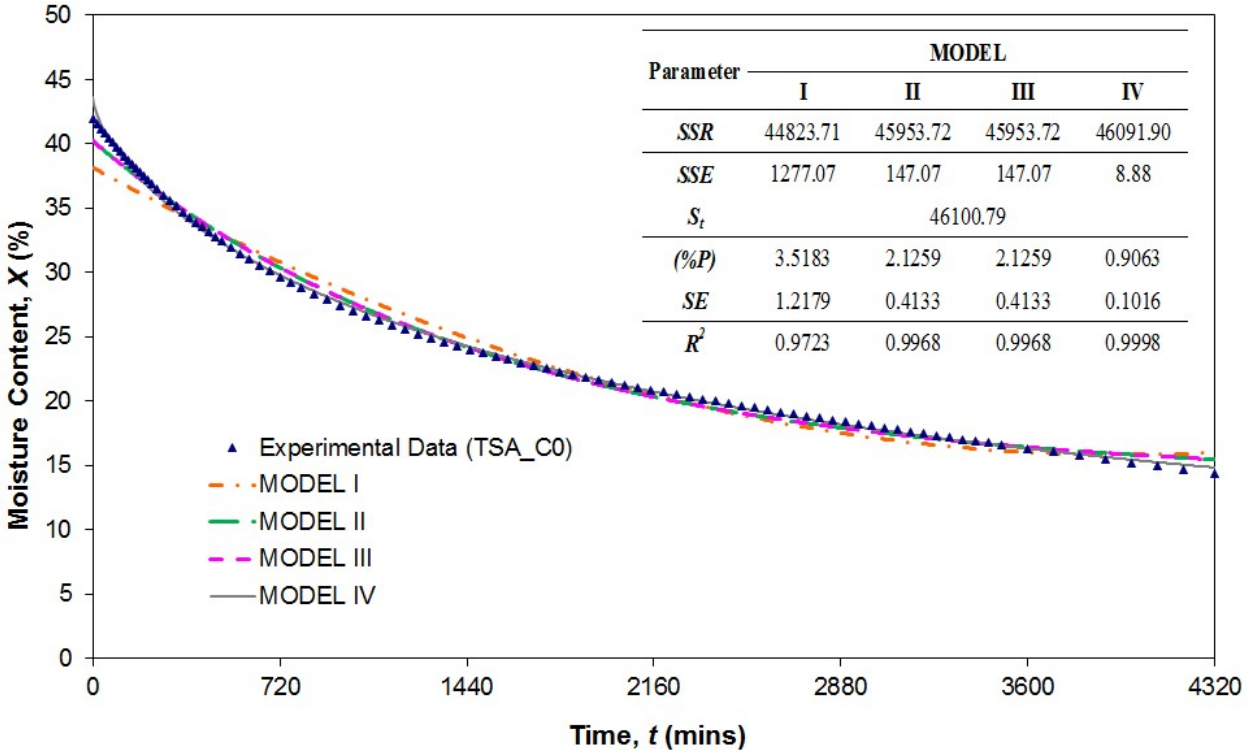

Parameter	MODEL			
	I	II	III	IV
SSR	44823.71	45953.72	45953.72	46091.90
SSE	1277.07	147.07	147.07	8.88
S_t	46100.79			
(%P)	3.5183	2.1259	2.1259	0.9063
SE	1.2179	0.4133	0.4133	0.1016
R^2	0.9723	0.9968	0.9968	0.9998

Fig. 2. Experimental moisture content for the TSA specimen versus time and its comparison with existent mathematical models.

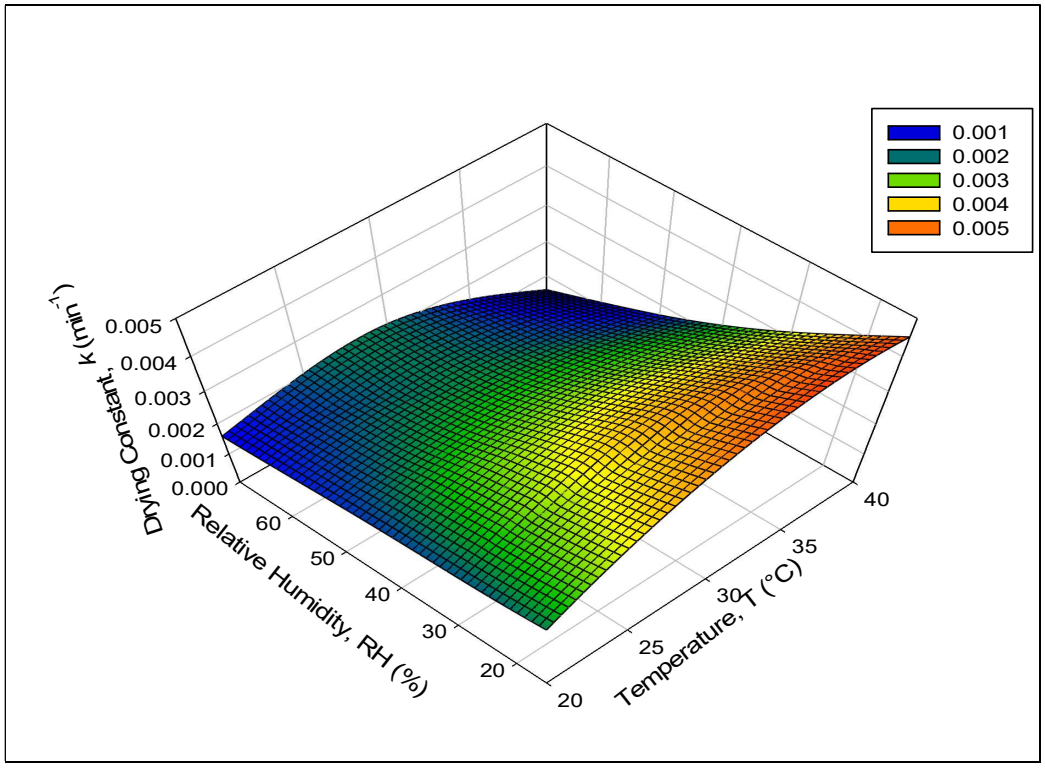

Fig. 3. Influence of Thermal Environment Condition on the Drying Constant k (TSA Specimen)

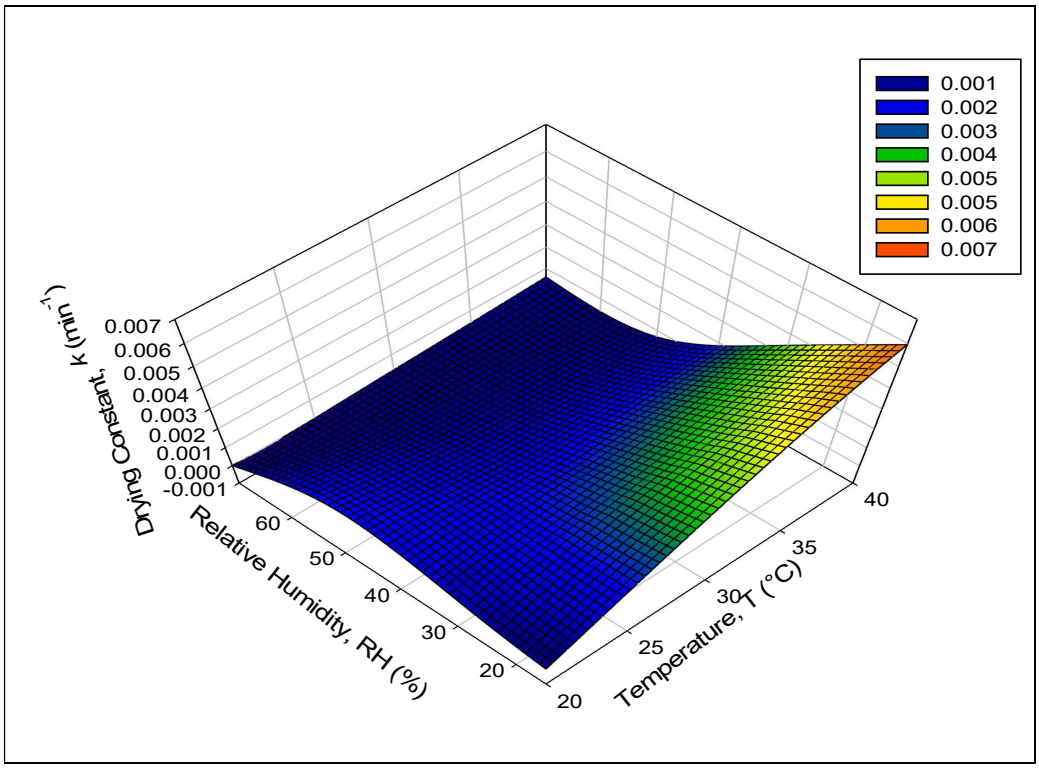

Fig. 4. Influence of Thermal Environment Condition on the Drying Constant k (TSB Specimen)

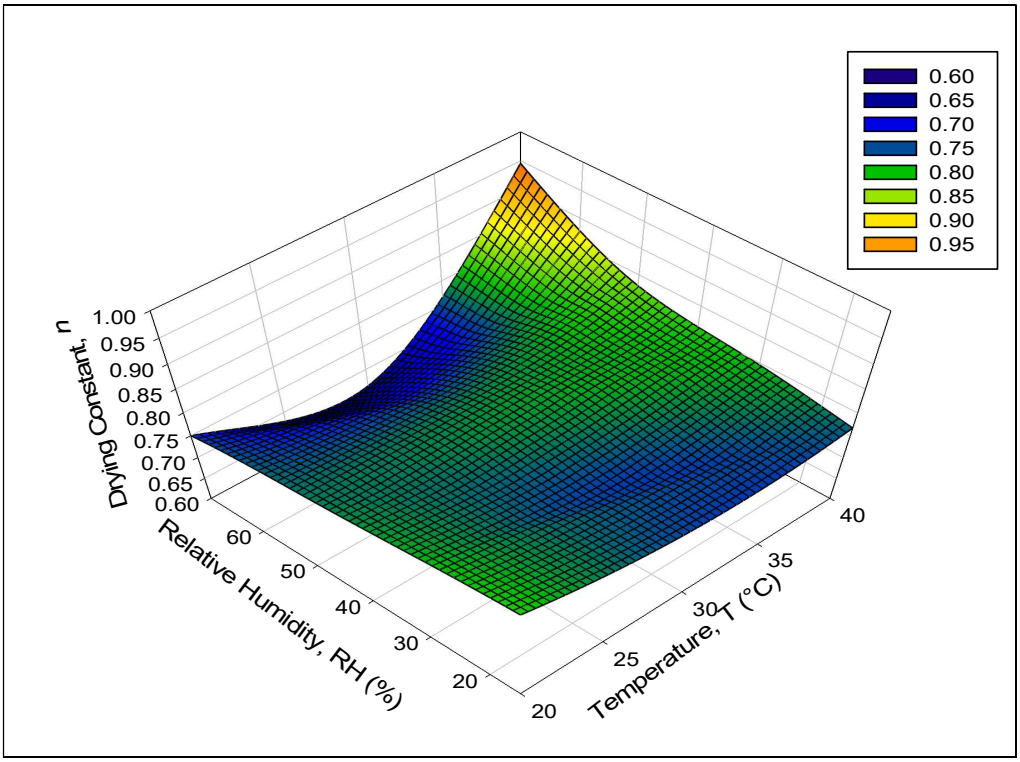

Fig. 5. Influence of Thermal Environment Condition on the Drying Constant *n* (TSA Specimen)

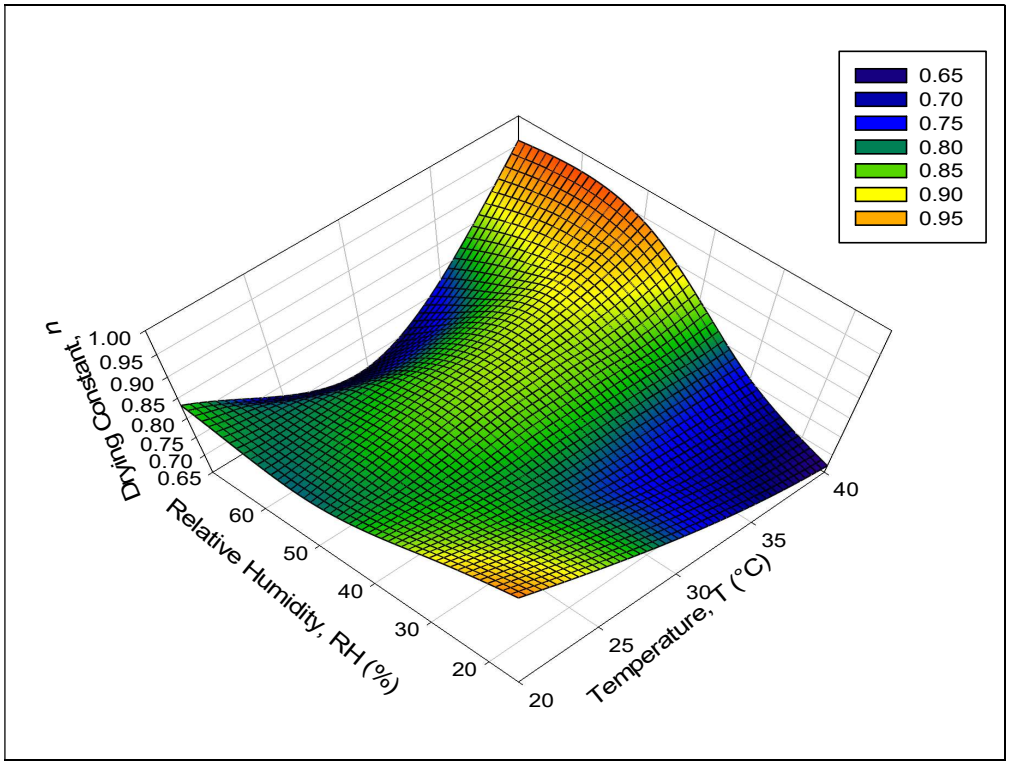

Fig. 6. Influence of Thermal Environment Condition on the Drying Constant *n* (TSB Specimen)

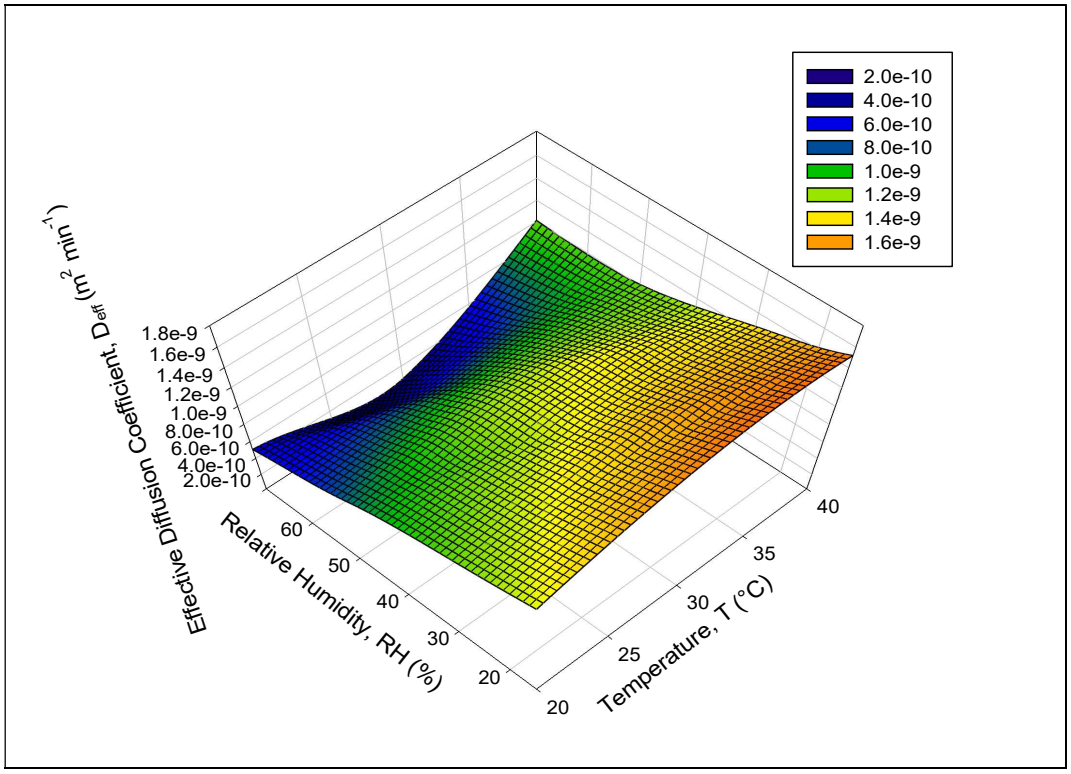

Fig. 7. Influence of Thermal Environment Condition on the Moisture Diffusion Coefficient, D_{eff} (TSA Specimen)

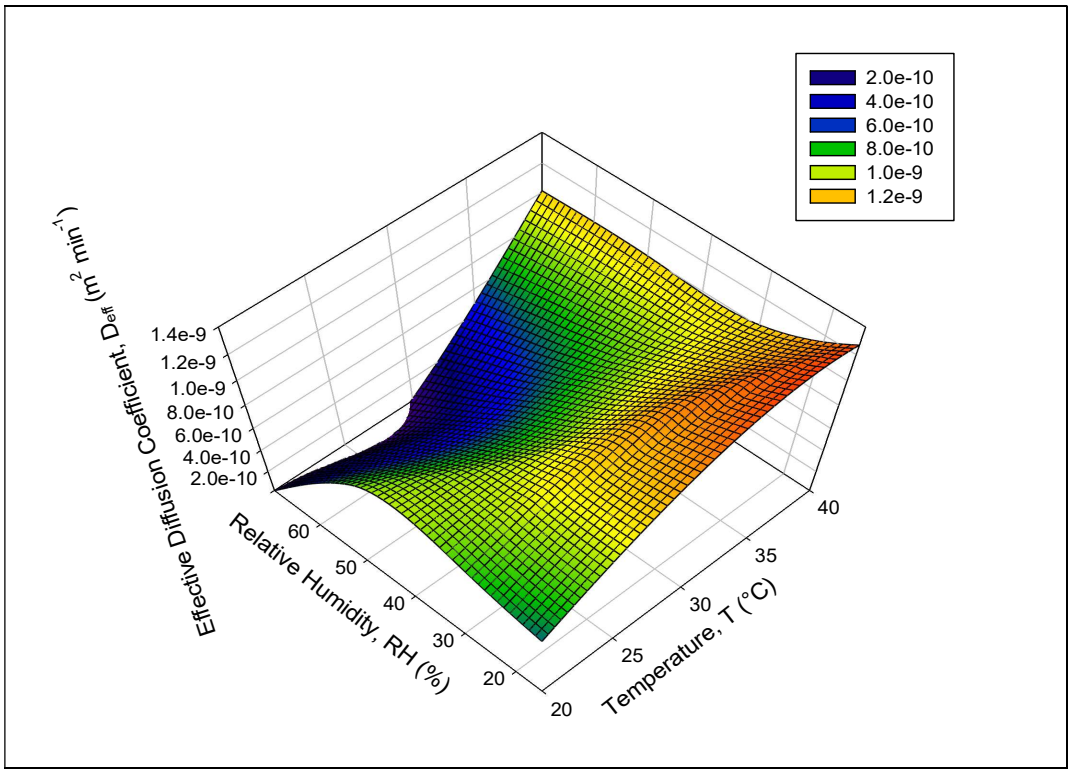

Fig. 8. Influence of Thermal Environment Condition on the Moisture Diffusion Coefficient, D_{eff} (TSB Specimen)

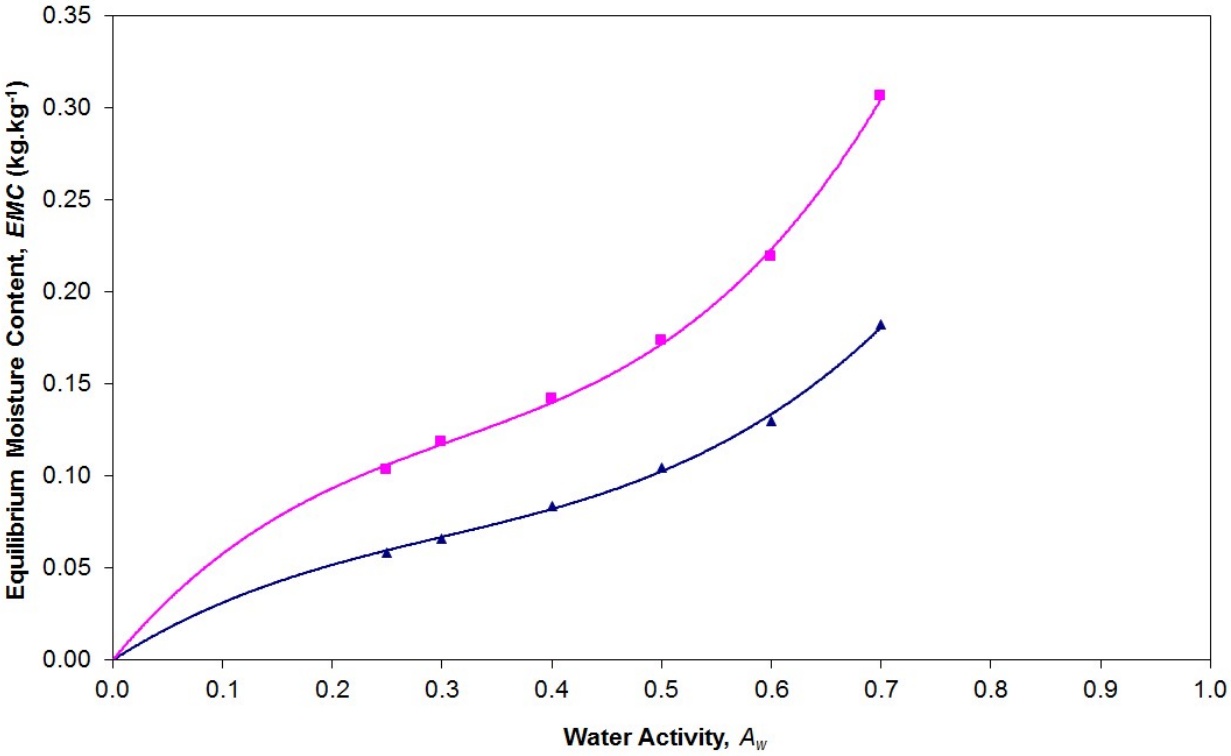

Fig. 9. Desorption isotherm of TSA Specimen (▲) and TSB Specimen (■) at 20°C

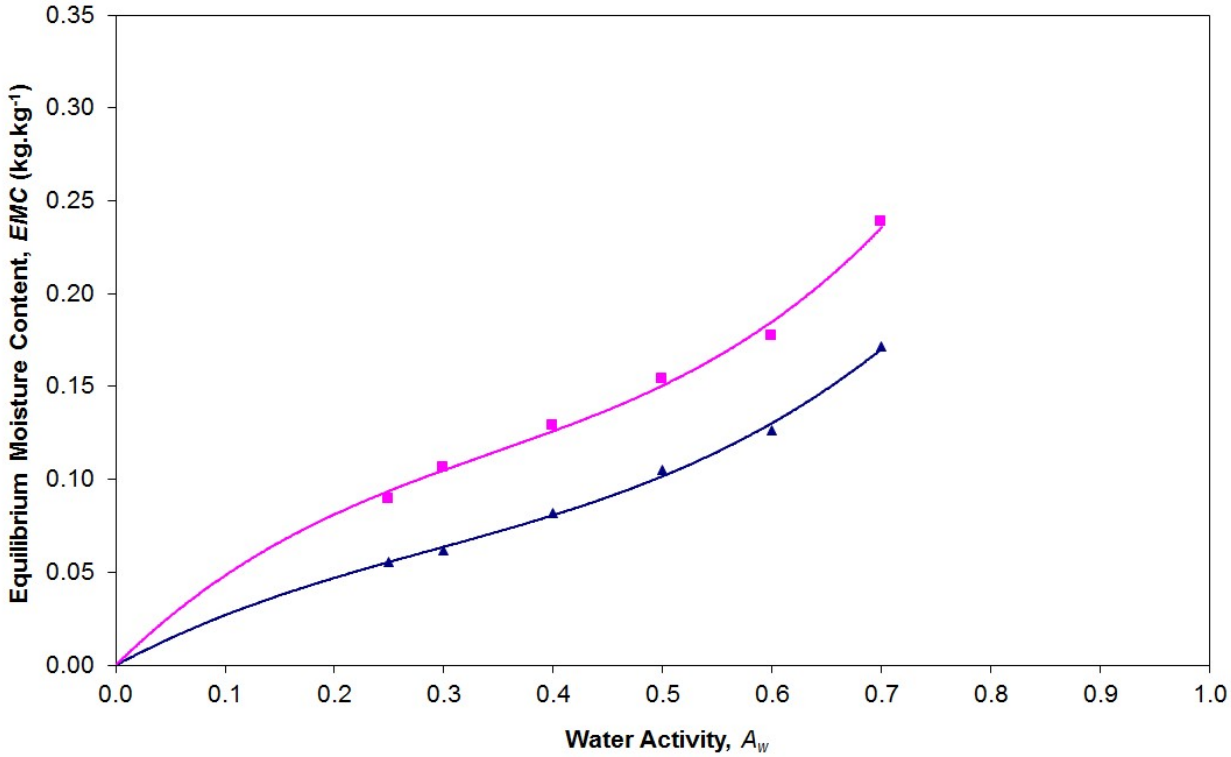

Fig. 10. Desorption isotherm of TSA Specimen (▲) and TSB Specimen (■) at 30°C

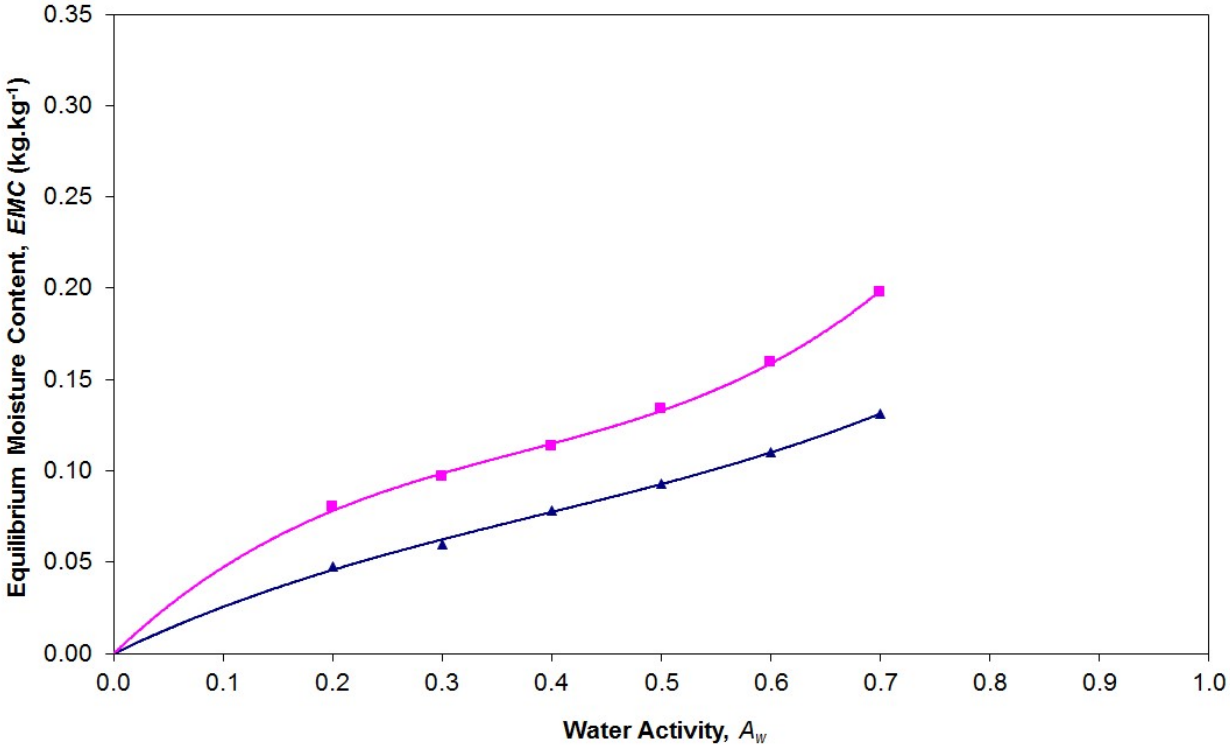

Fig. 11. Desorption isotherm of TSA Specimen (▲) and TSB Specimen (■) at 40°C

Table 1 Different thermal environments (combinations of Temperature & Relative humidity) used in this study

		Relative Humidity, RH (%)			
		15	**30**	**50**	**70**
Temperature, T (°C)	**20**	-	A1	A2	A3
	30	-	B1	B2	B3
	40	C0	C1	C2	C3

Table 2 Summary of quality fitting parameters for others thermal environment

TEST	MODEL	TSA			TSB		
		(%P)	SE	R^2	(%P)	SE	R^2
A1	I	1.3310	0.4940	0.9937	0.6164	0.3033	0.9972
	II	0.6151	0.2452	0.9984	0.7167	0.2737	0.9977
	III	0.6151	0.2452	0.9984	0.7167	0.2736	0.9977
	IV	0.3257	0.1036	0.9997	0.7267	0.2537	0.9980
A2	I	1.2277	0.4230	0.9952	0.9327	0.3370	0.9952
	II	0.6610	0.2372	0.9985	0.4888	0.1826	0.9986
	III	0.6610	0.2370	0.9985	0.4888	0.1825	0.9986
	IV	0.2815	0.0848	0.9998	0.2587	0.0870	0.9997
A3	I	0.8624	0.3279	0.9959	0.2753	0.1357	0.9982
	II	0.5771	0.2159	0.9982	0.2712	0.1324	0.9983
	III	0.5771	0.2157	0.9982	0.2712	0.1323	0.9983
	IV	0.2612	0.0946	0.9997	0.2343	0.1102	0.9988
B1	I	2.8458	0.8087	0.9852	1.6937	0.5311	0.9904
	II	1.1600	0.3411	0.9974	0.8057	0.2498	0.9979
	III	1.1600	0.3409	0.9974	0.8057	0.2497	0.9979
	IV	0.3605	0.0895	0.9998	0.4351	0.1368	0.9994
B2	I	2.0540	0.5821	0.9924	0.5380	0.2178	0.9982
	II	0.8806	0.2802	0.9982	0.3304	0.1381	0.9993
	III	0.8806	0.2801	0.9982	0.3304	0.1380	0.9993
	IV	0.3452	0.0884	0.9998	0.2565	0.0914	0.9997
B3	I	1.6127	0.5375	0.9939	0.5852	0.2348	0.9973
	II	1.2023	0.3794	0.9970	0.4899	0.1909	0.9982
	III	1.2023	0.3791	0.9970	0.4899	0.1908	0.9982
	IV	0.4048	0.1346	0.9996	0.1586	0.0648	0.9998
C0	I	5.4935	1.2179	0.9723	3.5183	0.9734	0.9794
	II	1.9354	0.4133	0.9968	201259	0.5307	0.9939
	III	1.9354	0.4131	0.9968	2.1259	0.5304	0.9939
	IV	0.5243	0.1016	0.9998	0.9063	0.2348	0.9988
C1	I	4.4237	0.9428	0.9826	3.2344	0.8833	0.9833
	II	1.4225	0.3255	0.9979	1.5827	0.3936	0.9967
	III	1.4225	0.3253	0.9979	1.5827	0.3934	0.9967
	IV	0.4620	0.0905	0.9998	0.7042	0.1814	0.9993
C2	I	2.9126	0.7773	0.9878	1.6518	0.5052	0.9929
	II	0.6543	0.2028	0.9992	7.5E-15	2.9E-14	1.0000
	III	0.6543	0.2027	0.9992	6.7E-15	2.9E-14	1.0000
	IV	0.3713	0.0995	0.9998	5.8E-15	2.9E-14	1.0000
C3	I	1.0065	0.3440	0.9963	0.4637	0.1973	0.9981
	II	8.0E-15	2.9E-14	1.0000	0.0708	0.0295	0.9999
	III	8.1E-15	2.9E-14	1.0000	0.0708	0.0295	0.9999
	IV	6.7E-15	2.9E-14	1.0000	0.0073	0.0031	1.0000

Table 3 Calculated value of constant and the statistical parameters for GAB sorption model to experimental desorption data of TSA and TSB specimens.

Parameter	TSA Specimen			TSB Specimen		
	20°C	30°C	40°C	20°C	30°C	40°C
X_m	0.0580	0.0662	0.0740	0.0898	0.0992	0.0741
C	9.8963	5.6319	6.9004	20.5160	10.0840	43.1684
K	0.9874	0.9415	0.7246	1.0000	0.8560	0.9051
$\%P$	1.0781	2.9019	1.5002	1.9612	2.7347	1.6915
SE	0.0025	0.0061	0.0018	0.0080	0.0070	0.00031
R^2	0.9982	0.9900	0.9980	0.9932	0.9900	0.9971